

V.Yu. Rozov, S.Yu. Reutskiy, D.Ye. Pelevin, K.D. Kundius

Magnetic field of electrical heating cable systems of the floors for residential premises

Problem. In order to effectively protect public health from the magnetic field of electric heating cable systems of the floors, it is necessary to reduce it to a safe level. However, this requires careful study of the magnetic field. **The purpose** of the work is to develop a mathematical model and a verified methodology for calculating the magnetic field of electric heating cable systems of the floors in residential premises, and assessment of compliance of the magnetic field with the normative level. **Method.** A methodology for calculating the magnetic field of electric heating cable systems of the floors in residential premises has been developed. **Scientific novelty.** Based on Bio-Savar's law and the principle of superposition, an analytical model of the magnetic field of electric heating cable systems of the floors and its calculation method was created. The magnetic field of the coaxial heating cable is determined, taking into account the value of its maximum eccentricity. The experimentally substantiated correctness of the obtained theoretical statements, which is confirmed by their coincidence with the results of the experiment with a spread of less than 7%. **Practical significance.** A verified methodology for calculating the magnetic field of electric heating cable systems of the floors was proposed and an assessment of compliance of their magnetic flux density with the normative level of $0.5 \mu\text{T}$ was performed. It is recommended to lay modern two-wire heating cables at a depth of at least 75–100 mm from the floor. With a smaller laying depth, it is recommended to use coaxial heating cables, which have an order of magnitude smaller magnetic field. References 51, tables 1, figures 11.

Key words: electric heating cable systems of the floors, magnetic field, modeling and measurement, assessment of compliance with the normative level.

Проблема. Для ефективного захисту здоров'я населення від магнітного поля кабельних систем електрообігріву підлог, необхідно його зменшення до безпечного рівня. Однак це потребує ретельного вивчення магнітного поля. **Метою роботи** є розробка математичної моделі і верифікованої методики розрахунку магнітного поля кабельних систем електрообігріву підлог житлових приміщень, та оцінка відповідності магнітного поля нормативному рівню. **Методика.** Розроблено методику розрахунку магнітного поля кабельних систем електрообігріву підлог в житлових приміщеннях. **Наукова новизна.** На основі закону Біо-Савара та принципу суперпозиції створено аналітичну модель магнітного поля кабельних систем електрообігріву підлог та методику його розрахунку. Визначено магнітне поле коаксіального нагрівального кабелю з урахуванням величини його максимального ексцентриситету. Експериментально обґрунтована коректність отриманих теоретичних положень, яка підтверджена їх співпадінням із результатами експерименту з розкидом менше 7%. **Практична значимість.** Запропоновано верифіковану методику розрахунку магнітного поля кабельних систем електрообігріву підлог і виконано оцінку відповідності індукції їх магнітного поля нормативному рівню $0,5 \text{ мкТл}$. Рекомендовано прокладати сучасні двожильні нагрівальні кабелі на глибині не менше $0,075\text{--}0,1 \text{ м}$ від підлоги. При меншій глибині прокладання рекомендовано використовувати коаксіальні нагрівальні кабелі, що мають на порядок менше магнітне поле. Бібл. 51, табл. 1, рис. 11.

Ключові слова: кабельні системи електрообігріву підлог, магнітне поле, моделювання та вимірювання, оцінка відповідності нормативному рівню.

Introduction. Safe and comfortable living of the population in residential buildings is impossible without limiting the level of man-made physical fields [1–3], including the electromagnetic field. One of the most powerful internal sources of electromagnetic field are electric heating cable systems (EHCSs) of floors [4, 5], which are now intensively distributed in the world. Also, like external power grids [6–8], EHCSs create quasi-stationary electromagnetic field of low frequency in residential premises, which is characterized by electric (EF) and magnetic (MF) components that negatively affect a person [6, 8–11]. According to the conclusions of the World Health Organization (WHO), the long-term effect of low frequency MF is more dangerous for public health than EF [12]. The basis for such a conclusion was the discovery at the end of the 20th century of the carcinogenic properties of MF of electrical networks with its weak but long-term effect on the population, and especially on children [13–16]. This led to the development by WHO experts of recommendations to limit the MF flux density of low frequency for the population with $100 \mu\text{T}$ [17] to the level of $0.2\text{--}0.3 \mu\text{T}$ to reduce the likelihood of cancer [18]. The level of MF flux density of low frequency that is comfortable for residential buildings is also recommended by the

international Standard [3] and is in the range of $0.02\text{--}0.5 \mu\text{T}$. The implementation of these recommendations led to the introduction of stricter national sanitary standards for the MF flux density with frequency of 50–60 Hz [19], stimulated the implementation of a complex of works on the development and implementation of new methods for determining and normalizing MF [3, 20–29].

In Ukraine, the solution of scientific problems of sanitary and hygienic regulation of MF for the population is carried out by the O.M. Marzeev Institute of Public Health of the National Academy of Medical Sciences of Ukraine (formerly the O.M. Marzeev Institute of Hygiene and Medical Ecology of the National Academy of Medical Sciences of Ukraine). In it, under scientific guidance of the famous in the world Ukrainian scientists and hygienists Academician A.M. Serdyuk and Professor [Yu.D. Dumanskyi], back in 1975, the need to introduce the maximum permissible level of MF flux density for the population was determined [30]. Finally, this normative for low frequency MF at the level of $0.5 \mu\text{T}$ was theoretically and experimentally (on animals) substantiated by them in [31]. It meets the current WHO recommendations and formed the scientific basis of the normative document adopted in 2017 [32], according to

© V.Yu. Rozov, S.Yu. Reutskiy, D.Ye. Pelevin, K.D. Kundius

which (Table 1) the effective value of MF flux density from cable lines at each point of the volume of the residential premises, including the floor (with the exception of the space closer to 0.5 m from the walls), should not exceed the safe level of $0.5 \mu\text{T}$.

Table 1

Temporary maximum permissible (normative) levels of the magnetic field above the path of the cable line according to Table 2.3.2 of the regulatory document of Ukraine «Electrical installation regulations» [32]

The territory on which the level of MF of the low frequency is regulated	MF flux density, μT
Inside residential premises	0,5
At a distance of 50 cm from the walls of residential premises and household electrical appliances	3,0* (*used for cables and wiring laid in walls)
On the territory of the residential development zone	10,0
Inhabited area outside the zone of residential development	20,0
Uninhabited area and agricultural land	50,0

The main elements of EHCS (Fig. 1) are resistive heating cables (HCs), which are mounted under the floor surface at a depth h_k from it, and a thermostat with a built-in temperature sensor [5]. HCs are powered by the apartment electrical network and are designed for a nominal current that can reach 15 A [4].

Analysis of the construct execution of HCs [5, 33–42] shows that they are divided into single-wire and two-wire (Fig. 2). Such HCs have different circuits of connection to the power grid (Fig. 3), and create different level of MF. According to [1, 43], the MF flux density of single-wire HCs significantly (more than an order of magnitude) exceeds the MF of two-wire HCs. This limits the use of single-wire HCs in non-residential premises.

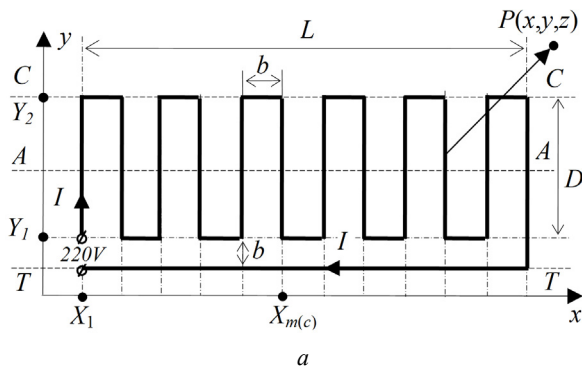


Fig. 3. Geometry of laying single-wire (a) and two-wire (b) EHCS HC in the horizontal plane XY under the floor and connection diagrams to the apartment electrical network

It is known that the MF flux density of two-wire HCs, like any electrical network, depends on the distance d between the axes of the wires and the current I in them [6, 8, 43]. Therefore, two-wire flat (planar) HCs (Fig. 2,b) are produced with the technologically minimum possible distance between its wires d (1.4–2.5 mm). However, as will be shown below, the use of such HCs at the standard depth of cable laying $h_k = 0.03\text{--}0.05$ m (Fig. 1) and a supply current of 10 A leads to a significant excess of MF flux density above the normative level of $0.5 \mu\text{T}$.

For uniform heating of the floor, HCs are laid in the form of a «snake» with a step of 80–120 mm [5]. This makes the distribution of EHCS MF different from the MF of single HCs, which determines its separate analysis. When analyzing the «snake» we present it in the form of a meander (Fig. 3).

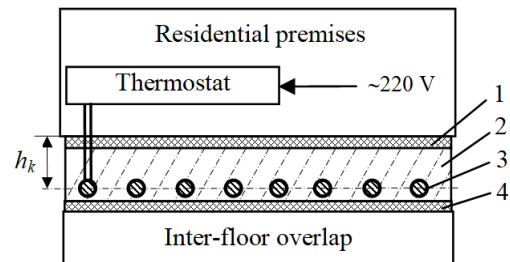


Fig. 1. Typical construction of an electrical heating cable systems (EHCS) (1 – floor covering, 2 – concrete (adhesive) screed, 3 – heating cable (HC), 4 – thermal insulation)

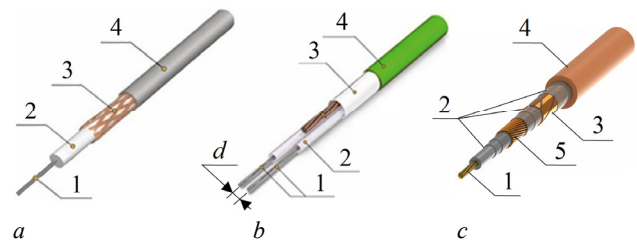


Fig. 2. Constructive implementation of HC of various types: single-wire (a), two-wire planar (b), two-wire coaxial (c); (1, 5 – heating (current-conducting) wires, 2 – electrical insulation, 3 – conductive grounding screen; 4 – external electrical insulation)

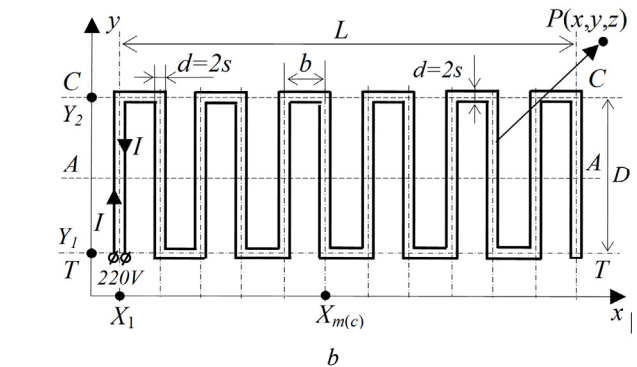


Fig. 3. Geometry of laying single-wire (a) and two-wire (b) EHCS HC in the horizontal plane XY under the floor and connection diagrams to the apartment electrical network

Normalization of the MF is possible when using coaxial [40] HCs (Fig. 2,c), but their MF has not been sufficiently investigated to date. Also, in well-known publications, for example [4, 42–45], the MF of EHCSs with various HCs is not sufficiently considered, there are no verified methods of calculating the MF of EHCSs, a correct assessment of the compliance of the MF flux density of their MF with the current regulations of Ukraine and authoritative international recommendations has not been performed.

The goal of the work is to develop a mathematical model and a verified methodology for calculating the

magnetic field of electric heating cable systems of the floors for residential premises, and assessment of compliance with the normative level.

Mathematical models of MF of rectilinear HCs.

When building the model, we will accept the following assumptions, which allow us to simplify the simulation, but do not significantly affect its result:

- the length L of the HC is significantly (by an order of magnitude) greater than the distance r to the observation point P , and also from the distance d between the wire axes of two-wire cables, which allows us to consider the HCs as infinitely;
- HCs are modelled by parallel rectilinear conducting wires in the form of current filaments located in horizontal planes;
- HC MF is potential and plane-parallel;
- the influence of external ferromagnetic (electrically conductive) elements and sources of MF of the residential premises, as well as the electrically conductive shield 3 (Fig. 2) of the HC is neglected;
- the voltage of the HC network power supply is sinusoidal.

Single-wire HC. According to the law of full current in integral form [46], the line integral of the strength H of the MF along a closed circuit is equal to the electric current I through the surface bounded by this circuit:

$$\oint_L (\mathbf{H}, d\mathbf{l}) = I. \quad (1)$$

Applying (1) to a circle lying on a plane with a radius r and centered at the point through which the infinity conductor passes, we obtain:

$$2\pi r H = I. \quad (2)$$

With the help of (2), we find the dependence of the strength of the MF of a single infinity conductor on its current, the coordinates of the conductor axis (x_c, y_c) and the coordinates of the observation point $P(x, y)$:

$$H(r) = \frac{I}{2\pi r^*}, \quad r^* = \sqrt{(x - x_c)^2 + (y - y_c)^2}. \quad (3)$$

From (3) under the conditions $x = r, y = 0$, we obtain the known [9, 46] relation that determines the flux density of the MF at a distance r from a single single-wire HC:

$$B_{OK} = \frac{\mu_0 I}{2\pi r}, \quad \mu_0 = 4\pi \cdot 10^{-7} \text{ H/m}. \quad (4)$$

Two-wire planar HC. It is obvious that the maximum value of MF flux density of a two-wire planar cable located in the horizontal plane XY with the distance between parallel wires d and the currents in them $\pm I$ is distributed along the vertical axis Z . In general, the problem of determining the MF of such a HC can be solved exclusively by numerical methods. However, if we consider the MF only along the Z axis, at a height r from the HC, then the task is significantly simplified due to symmetry. Applying Biot-Savart's law and elementary geometric constructions, similarly to [8], we obtain the following formula for calculating to the MF flux density module of a two-wire planar HC:

$$B_{DPK \max} = \frac{\mu_0}{2\pi} \frac{I \cdot d}{\left\{ r^2 + (0,5d)^2 \right\}}. \quad (5)$$

Two-wire coaxial HC. It is known that the MF of an infinity cylindrical conductor is equivalent to the MF of a filament with the same current passing through the axis of symmetry of such a conductor [10, 47]. Accordingly, in an ideal coaxial HC, the axes of both of its conductors (Fig. 2,c) coincide, and their currents are in different directions. Therefore, the MF of these currents is mutually compensated, and for an ideal coaxial HC, its resulting MF outside the conductors will be absent. But during the industrial production of HCs, technological deviations from the symmetrical shape arise. Here, the geometric axis inside the wire of the HC can shift by the value of eccentricity e [48, 49], which characterizes the value of its deviation from the axis of symmetry of the HC. The value of the technological dispersion of the eccentricity of coaxial cables during serial production can be 5–15 % (0.1–0.3 mm) of the ideal distance d between the axis of its central wire and the surface of the cylindrical conductive wire. Therefore, the external MF of a real coaxial HC will coincide with the MF of a conventional two-wire planar HC (5), in which the distance between its wires is equal to the eccentricity value ($d = e$). Taking into account the above, the MF flux density of a real coaxial HC on the basis of (5) can be determined by the relationships:

$$B_{DKK \max} = \frac{\mu_0}{2\pi} \frac{Ie}{\left\{ r^2 + (0,5e)^2 \right\}}. \quad (6)$$

Study of MF of different types of HC. We will use the obtained relationships (4)–(6) for the engineering calculation of the MF flux density of the HC as a function of the distance r to the observation point. Here, the value r corresponds to the depth h_k of the HC laying (Fig. 1), which determines the distance from the floor surface to the axis of the HC wires. The calculation results are presented in Fig. 4. The MF flux density of a single-wire HC at the manufacturer's recommended laying depth of 0.03–0.05 m [37–41] is 40–65 μT . This is 80–130 times higher than the normative level of 0.5 μT , which excludes the use of single-wire HCs in residential premises.

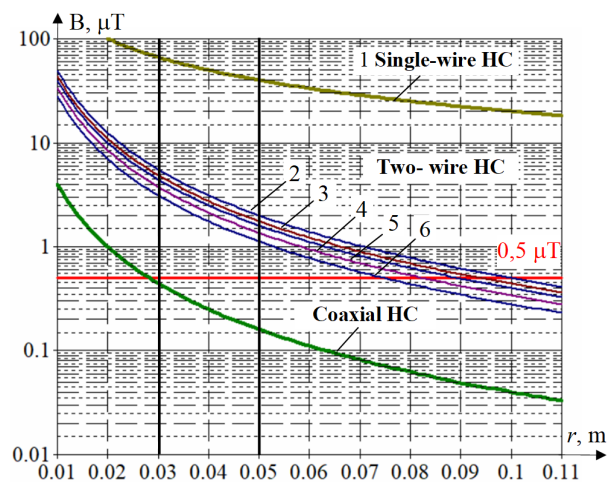


Fig. 4. Calculated values of flux density of MF of different types of rectilinear HCs when at a distance r along the Z axis (two-wire HCs with d : 2 – 2.5 mm; 3 – 2.2 mm; 4 – 2 mm; 5 – 1.7 mm; 6 – 1.4 mm; coaxial HC with $e = 0.2$ mm); $I = 10$ A

The MF flux density of two-wire HCs at a laying depth of 0.03–0.05 m, depending on the distance between

their wires d (Fig. 4) is from 2 to 5.5 μT , which exceeds the normative level of 0.5 μT by 4–11 times.

The MF flux density of the coaxial HC at $e = 0.2$ mm and the standard laying depth of 0.03–0.05 m is (Fig. 4) from 0.16 to 0.45 μT , which corresponds to the normative level of 0.5 μT . Therefore, coaxial HCs, with their eccentricity limited to $0.1d$ (approximately 0.2 mm), can be safely used in residential premises with a standard laying depth.

The results of calculating the MF flux density of real HCs are shown in Fig. 5. They are represented by a planar two-wire HC of the «Arnold Rak 6101-20 EC» type and a coaxial HC of the «Volterm» type at $e = 0.2$ mm and 0.05 mm (curves 2, 3), which was specially provided by the «VOLTERM» Company [40] for testing on the magnetometer stand of the Institute. Analysis of the calculation results (Fig. 5) shows that they correspond to the data in Fig. 4 and the above conclusions.

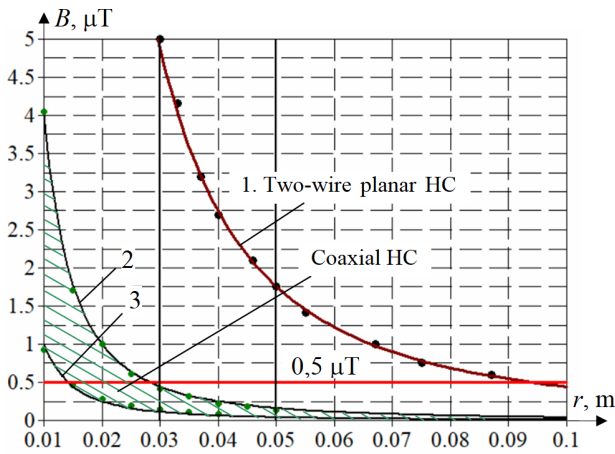


Fig. 5. Calculated — and experimental ●●● values of MF flux density of rectilinear two-wire planar HC type «Arnold Rak 6101-20 EC», $d = 2.2$ mm (1), as well as coaxial HC type «Volterm» (2, 3) with an eccentricity $e = 0.2$ –0.05 mm, when moving away from them by a distance r along the Z axis, $I = 10$ A

Now we will perform a study of the MF flux density distribution of the EHCS with different HCs by the scheme of their laying in accordance with Fig. 3. Such laying changes the spatial distribution of the EHCS MF in comparison with the MF of a single rectilinear HC due to the mutual influence of nearby conductors with a current behind the MF.

Mathematical model of EHCS MF. When building the MF model, we accept the following assumptions: EHCS HCs are modeled by a broken line (meander, Fig. 3) of rectilinear parallel current filaments located in the horizontal plane; quasi-stationary EHCS MF is three-dimensional; the influence of external ferromagnetic (electrically conductive) elements and sources of MF are neglected; the power supply voltage is sinusoidal.

We will perform the simulation using an analytical method based on Biot-Savard's law and the principle of superposition [9, 10, 46, 47] by determining the result in the form of a vector sum of the MF flux density at the observation point $P(x, y, z)$ from individual current-carrying conductors.

At a point with a radius vector \mathbf{R} , a contour element $d\mathbf{r}$ with a current I generate a MF with MF flux density:

$$d\mathbf{B}(t) = \frac{\mu_0 I}{4\pi R^3} [d\mathbf{r} \times \mathbf{R}], \quad (7)$$

where the vector \mathbf{R} is directed from the location point of the contour element $d\mathbf{r}$ to the observation point $P(x, y, z)$. The total MF of the contour C has the MF flux density:

$$\mathbf{B} = \frac{\mu_0 I}{4\pi} \int_C \frac{[d\mathbf{r} \times \mathbf{R}]}{R^3}. \quad (8)$$

Consider the MF (Fig. 6,a) created by the current I , which passes through a straight section between the points $A_n(X_0, Y_1, 0)$ and $A_k(X_0, Y_2, 0)$, i.e., the segment with the current located in the plane $z = 0$ parallel to the y axis at a distance X from the y axis (Fig. 6,a). In this case, the contour element is equal to:

$$d\mathbf{r} = d\eta \mathbf{e}_y, \quad Y_1 \leq \eta \leq Y_2, \quad (9)$$

and its coordinates:

$$(X_0, \eta, 0), \quad Y_1 \leq \eta \leq Y_2. \quad (10)$$

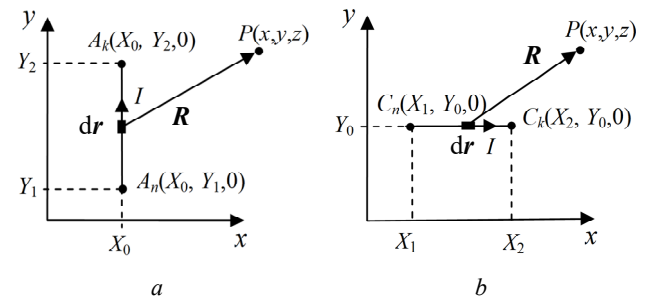


Fig. 6. To determination of the MF flux density of segments with a current located parallel to the y (a) and x (b) axes

Then the vector directed from the point where the current element $d\mathbf{r}$ is located to the observation point $P(x, y, z)$ is equal to:

$$\mathbf{R} = (x - X_0, y - \eta, z).$$

The third degree of the distance between the contour element and the observation point:

$$R^3 = [(x - X_0)^2 + z^2 + (y - \eta)^2]^{3/2}. \quad (11)$$

Vector product:

$$[d\mathbf{l} \times \mathbf{R}] = \begin{vmatrix} \mathbf{e}_x & \mathbf{e}_y & \mathbf{e}_z \\ 0 & d\eta & 0 \\ x - X_0 & y - \eta & z \end{vmatrix} = zd\eta \mathbf{e}_x - (x - X_0)d\eta \mathbf{e}_z. \quad (12)$$

The MF flux density components of a rectilinear segment with current will be written as:

$$B_x = \frac{\mu_0 I}{4\pi} z \int_{Y_1}^{Y_2} \frac{d\eta}{R^3}; \quad B_y = 0; \quad B_z = -\frac{\mu_0 I}{4\pi} (x - X_0) \int_{Y_1}^{Y_2} \frac{d\eta}{R^3}. \quad (13)$$

In [50] there is a formula for the indefinite integral:

$$\int \frac{dt}{T(t)^{3/2}} = \frac{4at + 2b}{(4ac - b^2)T(t)^{1/2}}; \quad T(t)^{1/2} = [c + bt + at^2]^{1/2}. \quad (14)$$

Using it, we calculate the integral in (13):

$$\int_{Y_1}^{Y_2} \frac{d\eta}{R^3} = \int_{Y_1}^{Y_2} \frac{d\eta}{[(x - X_0)^2 + z^2 + (y - \eta)^2]^{3/2}} =$$

$$\begin{aligned}
&= \int_{Y_1}^{Y_2} \frac{d\eta}{[c+(y-\eta)]^{3/2}} = \int_{Y_1}^{Y_2} \frac{d\eta}{[c+(\eta-y)]^{3/2}} = \\
&= \int_{Y_1-y}^{Y_2-y} \frac{dt}{[c+t^2]^{3/2}} = \left[\frac{1}{c} \frac{t}{[c+t^2]^{1/2}} \right]_{Y_1-y}^{Y_2-y} = \\
&= \frac{1}{(x-X_0)^2+z^2} \left[\frac{Y_2-y}{[(x-X_0)^2+z^2+(Y_2-y)^2]^{1/2}} - \right. \\
&\quad \left. - \frac{Y_1-y}{[(x-X_0)^2+z^2+(Y_1-y)^2]^{1/2}} \right]. \quad (15)
\end{aligned}$$

We denote:

$$F(X_0, Y) = \frac{Y-y}{\left((x-X_0)^2+z^2 \right) \left[(x-X_0)^2+z^2+(Y-y)^2 \right]^{1/2}}.$$

Then the components of the MF will be written in the form:

$$\begin{aligned}
BY_x(X_0, Y_1, Y_2) &= \frac{\mu_0 I}{4\pi} z [F(X_0, Y_2) - F(X_0, Y_1)]; \\
BY_z(X_0, Y_1, Y_2) &= -\frac{\mu_0 I}{4\pi} (x-X_0) [F(X_0, Y_2) - F(X_0, Y_1)]; \\
BY_y(X_0, Y_1, Y_2) &= 0. \quad (16)
\end{aligned}$$

The functions $BY_x(X_0, Y_1, Y_2)$, $BY_y(X_0, Y_1, Y_2)$, $BY_z(X_0, Y_1, Y_2)$ give the components of the MF flux density of a conductor segment parallel to the y axis with a current I at a distance X_0 from the axis.

Consider the MF in the direction of the x axis from the current I passing along the segment between the points $C_n(X_1, Y_0, 0)$ and $C_k(X_2, Y_0, 0)$ (Fig. 6,b). The segment with the current is located in the $z = 0$ plane, passes parallel to the x axis at a distance Y_0 from the x axis. Performing calculations similar to (9)–(14), we obtain:

$$\begin{aligned}
BX_y(Y_0, X_1, X_2) &= -\frac{\mu_0 I}{4\pi} z [G(X_2, Y_0) - G(X_1, Y_0)]; \\
BX_z(Y_0, X_1, X_2) &= \frac{\mu_0 I}{4\pi} (y-Y_0) [G(X_2, Y_0) - G(X_1, Y_0)]; \\
BX_x(Y_0, X_1, X_2) &= 0, \quad (17)
\end{aligned}$$

where

$$G(X, Y_0) = \frac{X-x}{\left((y-Y_0)^2+z^2 \right) \left[(y-Y_0)^2+z^2+(X-x)^2 \right]^{3/2}}.$$

The functions $BX_x(Y_0, X_1, X_2)$, $BX_y(Y_0, X_1, X_2)$, $BX_z(Y_0, X_1, X_2)$ give the spatial components of the MF flux density of a conductor segment parallel to the x axis with a current I at a distance Y_0 from the axis.

We will use (16), (17) to determine the calculation relationships of MF of real EHCS of floors, the cable laying schemes for which are presented in Fig. 3.

Calculation relationships for EHCS MF with single-wire HC. The MF flux density at point P from the system of single-wire conductors (Fig. 3,a) in the plane $z = \text{const}$, which are parallel to the x and y coordinate axes, is determined by the vector sum of the MF flux density from their straight line segments. Then, according to (16), (17), the components of EHCS MF can be represented as:

$$\begin{aligned}
B_x &= \sum_{m=1}^{m=K/2} [BY_x(X_{2m-1}, Y_1, Y_2) + BY_x(X_{2m}, Y_2, Y_1)] + \\
&\quad + BY_x(X_K, Y_1, Y_1 - b); \\
B_y &= \sum_{c=1}^{c=K/2-1} [BX_y(Y_2, X_{2c-1}, X_{2c}) + BX_y(Y_1, X_{2c}, X_{2c+1})] + \\
&\quad + BX_y(Y_2, X_{K-1}, X_K) + BX_y(Y_1 - b, X_K, X_1); \\
B_z &= \sum_{m=1}^{m=K/2} [BY_z(X_{2m-1}, Y_1, Y_2) + BY_z(X_{2m}, Y_2, Y_1)] + \\
&\quad + BY_z(X_K, Y_1, Y_1 - b) + \\
&\quad + \sum_{c=1}^{c=K/2-1} [BX_z(Y_2, X_{2c-1}, X_{2c}) + BX_z(Y_1, X_{2c}, X_{2c+1})] + \\
&\quad + BX_z(Y_2, X_{K-1}, X_K) + BX_z(Y_1 - b, X_K, X_1), \quad (18)
\end{aligned}$$

where $X_m, Y_{1,2}, K$ are the coordinates of the ends and the number of segments parallel to the y axis; $X_c, Y_{1,2}$ are the coordinates of the ends of segments parallel to the x axis.

The effective value of the MF flux density of EHCS at the point $P(x, y, z)$ is defined as:

$$\tilde{B}(P) = \sqrt{B_x^2 + B_y^2 + B_z^2}, \quad (19)$$

where the spatial components B_x, B_y, B_z are obtained according to (18).

Calculation relationships for EHCS MF with two-wire HC. The MF flux density at the point $P(x, y, z)$ from the system of two-wire conductors (Fig. 3,b) with a distance between the axes of the wires $d = 2s$, laid out in the plane $z = \text{const}$ parallel to the x and y coordinate axes, is determined by the sum of the MF from their rectilinear segments. Then, according to (16), (17), the components of MF flux density of EHCS with two-wire HC can be represented in the form:

$$\begin{aligned}
B_x &= \sum_{m=1}^{m=K/2} [BY_x(X_{2m-1} - s, Y_1 + s, Y_2 + s) + \\
&\quad + BY_x(X_{2m} + s, Y_2 + s, Y_1 + s) + \\
&\quad + BY_x(X_{2m-1} + s, Y_2 - s, Y_1 - s) + \\
&\quad + BY_x(X_{2m} - s, Y_1 - s, Y_2 - s)] + \\
&\quad + BY_x(X_K + s, Y_1 + s, Y_1 - s); \\
B_y &= \sum_{c=1}^{c=K/2-1} [BX_y(Y_2 + s, X_{2c-1} - s, X_{2c} + s) + \\
&\quad + BX_y(Y_1 + s, X_{2c} + s, X_{2c+1} - s) + \\
&\quad + BX_y(Y_2 - s, X_{2c} - s, X_{2c-1} + s) + \\
&\quad + BX_y(Y_1 - s, X_{2c+1} + s, X_{2c} - s)] + \\
&\quad + BX_y(Y_2 + s, X_{K-1} - s, X_K + s) + \\
&\quad + BX_y(Y_2 - s, X_K - s, X_{K-1} + s) + \\
&\quad + BX_y(Y_1 - s, X_K + s, X_K - s); \\
B_z &= \sum_{m=1}^{m=K/2} [BY_z(X_{2m-1} - s, Y_1 + s, Y_2 + s) + \\
&\quad + BY_z(X_{2m} + s, Y_2 + s, Y_1 + s) + \\
&\quad + BY_z(X_{2m-1} + s, Y_2 - s, Y_1 - s) +
\end{aligned}$$

$$\begin{aligned}
& + BY_z(X_{2m} - s, Y_1 - s, Y_2 - s)] + \\
& + BY_z(X_K + s, Y_1 + s, Y_1 - s_1) + \\
& + \sum_{c=1}^{c=K/2-1} [BX_z(Y_2 + s, X_{2c-1} - s, X_{2c} + s) + \\
& + BX_z(Y_1 + s, X_{2c} + s, X_{2c+1} - s) + \\
& + BX_z(Y_2 - s, X_{2c} - s, X_{2c-1} + s) + \\
& + BX_z(Y_1 - s, X_{2c+1} + s, X_{2c} - s)] + \\
& + BX_y(Y_2 + s, X_{K-1} - s, X_K + s) + \\
& + BX_y(Y_2 - s, X_K - s, X_{K-1} + s) + \\
& + BX_y(Y_1 - s, X_K + s, X_K - s). \quad (20)
\end{aligned}$$

The effective value of MF flux density is determined from (19).

The obtained relationships (18)–(20) make it possible to calculate the MF flux density distribution of EHCS in the case of performing their HC from straight segments – in the form of a rectangular meander (Fig. 3). However, the actual form of HC decomposition can be performed both from practically rectilinear segments [33] and in the form of a «snake» [35] with a radius of curvature of the HC at the level of $0.5b$ (Fig. 10) or less. Outside of the scope of this article, the authors have studied the influence of the shape of decomposition of the top of the HC on the level of EHCS MF, and it is shown that the decomposition in the form of a rectangular meander (Fig. 3) gives the maximum values of MF. This is confirmed by verified curves 1, 3 in Fig. 8, 9. This makes it possible to use the proposed relationships (18)–(20) as universal ones, without taking into account the shape of the peaks of the expansion, to determine the MF flux density of EHCS in the worst case.

Study of EHCS MF with HC of different types.

We will use relationships (18)–(20) to determine the MF flux density of EHCS with single-wire and two-wire HCs. Here, we mean that the maximum MF flux density values of the potential EHCS MF in the entire volume of the premises are concentrated on its floor.

Figure 7 presents a map of the distribution of MF over the EHCS with a single-wire HC, made with dimensions of 1.2×0.8 m and a step of 0.1 m (Fig. 3,a). The maximum level of MF flux density ($42 \mu\text{T}$) occurs at

the top of the meander (Fig. 3,a) – on the CC line, and above the return wire (TT line). These values practically coincide with the MF of a single rectilinear HC (Fig. 4), which allows us to estimate the maximum values of the MF of this EHCS according to relationship (4). In connection with the significant excess of the normative level of MF, the EHCS with a single-wire HC will not be considered below.

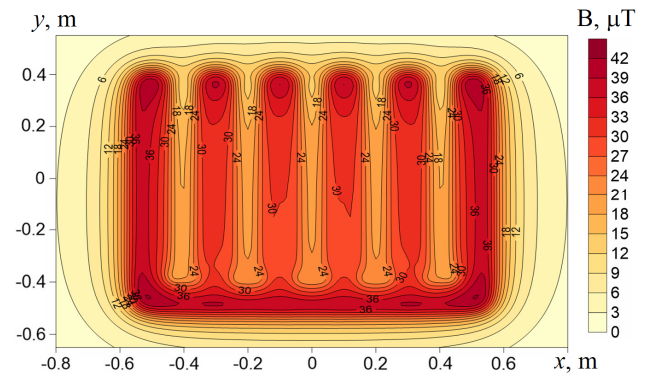


Fig. 7. Calculated values of the MF flux density distribution from EHCS with a single-wire HC type Fenix ASL1P 18 on the floor surface at $h_k = 0.05$ m, $I = 10$ A

The calculated distribution map of EHCS MF with an industrial sample of a two-wire planar HC (Fig. 3,b) at $h_k = 0.05$ m with $d = 2.2$ mm is presented in Fig. 8,a. Figure 8,b shows characteristic graphical dependencies. As can be seen from Fig. 8, the maximum values of the MF flux density of EHCS are $2.16 \mu\text{T}$. They take place at the top of the decomposition – along the TT and CC lines (Fig. 3,b). These values are greater than the MF of a single HC (Fig. 4) by approximately 15 %.

The calculated distribution map of EHCS MF with an industrial sample of coaxial HC with $e = 0.2$ mm at $h_k = 0.05$ m, made according to Fig. 3,b, is presented in Fig. 9,a. Figure 9,b shows the calculated graphic dependencies. As can be seen from Fig. 9, the maximum values of the MF flux density of EHCS are $0.196 \mu\text{T}$, which is significantly less than the normative level of $0.5 \mu\text{T}$.

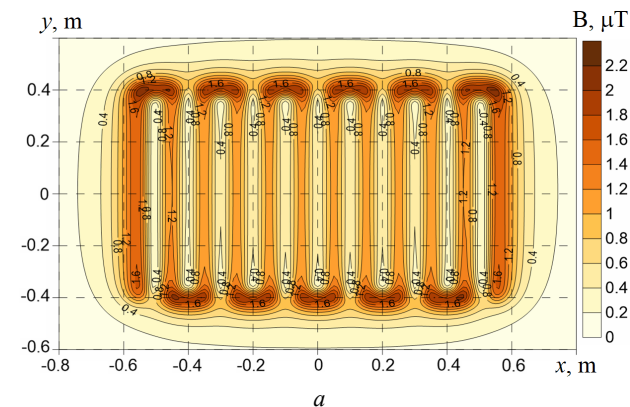


Fig. 8. Distribution of MF from EHCS with a two-wire planar HC type Arnold Rak 6101-20 EC ($I = 10$ A, $d = 2.2$ mm) on the floor surface at $h_k = 0.05$ m (EHCS with a rectangular decomposition of HC (Fig. 3,b): 1 – along the CC line; 2 – along the AA line); 3 – EHCS with the «snake» decomposition of HC (Fig. 10) along the CC line (Fig. 3,b), (— calculation ••• experiment)

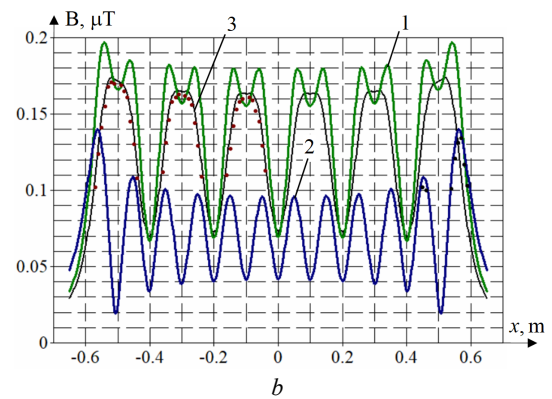
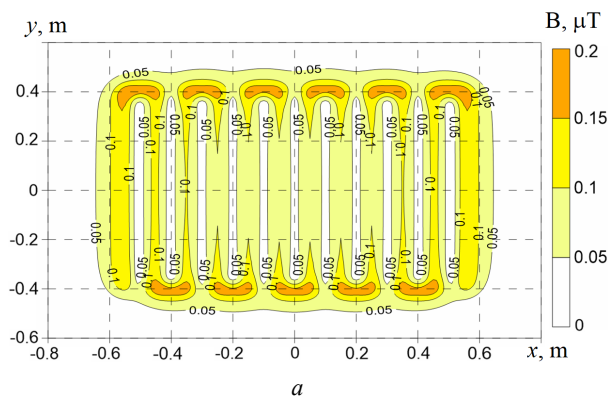


Fig. 9. Distribution of MF from EHCS with coaxial HC type «Volterm HR18» ($I = 10$ A, $e = 0.2$ mm) on the surface of the floor at $h_k = 0.05$ m (EHCS with a rectangular decomposition of HC (Fig. 3,b): 1 – along the CC line; 2 – along the AA line); 3 – EHCS with the «snake» decomposition of HC (Fig. 10) along the CC line (Fig. 3,b), (— calculation ••• experiment)

Experimental studies of MFs of various types of HC and EHCS based on them. The research was carried out on industrial samples of HC and laboratory models of EHCS based on them at the unique magnetic measuring stand of IPMach of the National Academy of Sciences of Ukraine [26, 27]. Industrial samples of a two-wire planar HC type «Arnold Rak 6101-20 EC» and a coaxial HC type «Volterm HR18» were studied, as well as laboratory models of EHCS based on them, made in accordance with Fig. 3 with dimensions of 1.2×0.8 m and decomposition of the HC with a step of 0.1 m with a snake (Fig. 10). MF flux density measurements were carried out with a certified vector magnetometer type Magnetoscop 1.069 of the Foerster Company (MF flux density measurement range 1 nT–600 mT, error 2.5 %).

Measurement of MF of individual HCs. The results of MF flux density measurements are presented in Fig. 5. For a planar HC, the spread of calculation and experiment results does not exceed 5 %, which confirms the correctness of the developed mathematical models and calculation relationships (18)–(20).

In the process of experimental studies of the «Volterm HR18» type coaxial HC, the inhomogeneity of the distribution of MF flux density along its length was revealed, which at $r = 0.03$ m varies from $0.16 \mu\text{T}$ to $0.44 \mu\text{T}$. Here, the maximum values of MF flux density according to (6) correspond to the value of eccentricity e at the level of 0.2 mm, and the minimum values of e at the level of 0.05 mm. The spread of the experimental values of the MF flux density by the length of this HC is presented in Fig. 5 in the form of a shaded area between curves 2 and 3. It is significant and indicates the instability of the eccentricity of this HC, which indicates the need to improve the production technology of the coaxial HC by the «Volterm» Company.

Measurement of EHCS MF. Measurements of the MF flux density of EHCS were performed on their laboratory mock-ups (Fig. 10) with the indicated types of HCs. The measurement results are presented in Fig. 8, 9. The spread of calculation and experiment results does not exceed 7 %.

The largest spread occurs at the tops of the EHCS (lines CC, Fig. 3,b), which is associated with the difference in the shape of the top of the mock-up (semicircle, Fig. 10) and the calculation model (rectangle,

Fig. 3). However, the spread of the experimental results in comparison with the additionally performed calculation of the MF flux density EHCS by the authors for the case of decomposition of the EHCS vertices according to Fig. 10 in the form of a semicircle with a radius of 50 mm (curve 3 in Fig. 8, 9), also does not exceed 7 %. Therefore, the results of the experiment fully confirm the correctness of the developed mathematical models of EHCS MF (7)–(17) and relations (18)–(20) obtained on their basis.



Fig. 10. Study of the distribution of MF flux density of the EHCS laboratory model with a coaxial HC of the «VOLTERM» type on the magnetometer stand of IPMach of the National Academy of Sciences of Ukraine

Assessment of compliance of EHCS MF with the normative level. On the basis of the verified calculation relationships(18)–(20), the calculation of the maximum values of MF flux density, created by EHCS with modern two-wire planar HCs with d from 1.4 to 2.5 mm and coaxial HCs with eccentricity $e = 0.2$ mm and $e = 0.1$ mm eas carried out. The calculation was performed on the surface of the floor of the living premise at different depth h_k of laying the HC and a current of 10 A. The results of the calculation in the form of graphs are presented in Fig. 11.

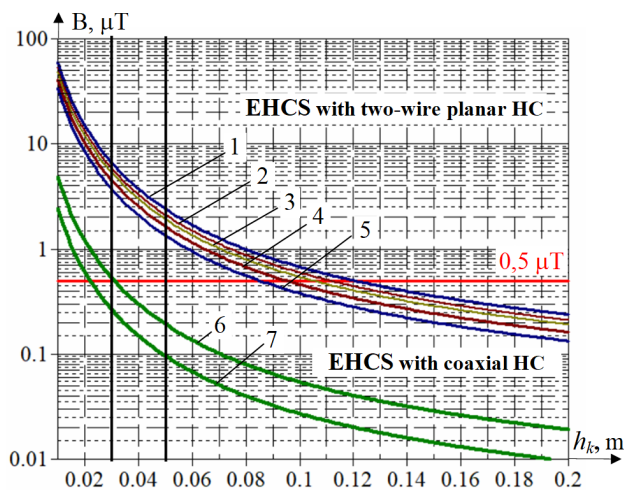


Fig. 11. Calculated by the verified relationships (19), (20) the maximum flux density values of EHCS MF created on the surface of the floor with two-wire planar HCs (d : 1 – 2.5 mm; 2 – 2.2 mm; 3 – 2 mm; 4 – 1.7 mm; 5 – 1.4 mm) and coaxial HCs (6 – $e = 0.2$ mm; 7 – $e = 0.1$ mm) with different depth of their laying h_k , $I = 10$ A

Analysis of Fig. 11 allows us to state the following. When performing EHCS on the basis of modern two-wire HCs with a minimum distance between wires of 1.4 mm, the maximum value of MF flux density on the floor of residential premises is 3.75–1.3 μT with a laying depth of 0.03–0.05 m and a current of 10 A. This is 7.5–2.6 times higher than the maximum permissible level of MF flux density of 0.5 μT . Therefore, the safe use of EHCS based on modern two-wire HCs is achieved only when their laying depth is more than 0.085–0.1 m, or in the case of limiting their current and, accordingly, thermal power.

The reduction of EHCS MF is also possible by installing between the EHCS and the floor of the room a continuous electromagnetic shield, for example, made of welded conductive aluminum sheets 1.5–2 mm thick. But with the expected MF shielding factor at the level of 1.5–2.5 units [51], the cost of such a shield will exceed the cost of EHCS.

Performing EHCS on the basis of coaxial HCs with an eccentricity $e \leq 0.2$ mm at a laying depth of 0.03–0.05 m allows to reduce their MF flux density to the normative level of 0.5 μT . Therefore, the widespread introduction of coaxial HCs is an effective method of solving the problem of reducing possible risks to the health of the population and ensuring their comfortable living in residential premises.

It is also advisable to further improve the design and production technology of coaxial HCs to limit their maximum eccentricity to 0.1 mm and ensure its stability in operating conditions.

Conclusions.

1. On the basis of the Bio-Savar's law and the principle of superposition, an analytical model of the magnetic field of electric heating cable systems of the floors for residential premises and a methodology for calculating the magnetic flux density based on it have been developed.

2. Verification of the developed mathematical model and technique of calculating the magnetic field was carried out through experimental studies of laboratory

layouts of electric heating cable systems with industrial samples of various types of heating cables. The measurements confirmed the coincidence of the results of the calculation and the experiment with a spread of no more than 7%.

3. The magnetic field of the coaxial heating cable was studied and the method of its calculation was proposed, taking into account the maximum value of the eccentricity of its central wire.

4. An assessment of the compliance of the magnetic field in the residential premises with the normative level of 0.5 μT when using electric heating cable systems with different heating cables was carried out, and based on which:

a) an excess of the maximum permissible level of magnetic flux density on the floor of residential premises by 2.6–7.5 times was found when using modern two-wire planar heating cables with a minimum distance between the wire of 1.4 mm at the depth of their laying of 0.05–0.03 m and a current of 10 A;

b) it is shown that the safe use in residential premises of modern planar two-wire heating cables with a current of 10 A requires an increase in the depth of their laying to 0.085–0.1 m.

c) to reduce possible risks to the health of the population and ensure their comfortable living, it is recommended to use coaxial heating cables in residential premises, which create an order of magnitude smaller magnetic field than modern two-wire planar heating cables.

Conflict of interest. The authors declare no conflict of interest.

REFERENCES

1. Brune D., Hellborg R., Persson B.R.R., Pääkkönen R. Radiation at home, outdoors and in the workplace. *Scandinavian Science Publisher*, 2001, 547 p.
2. *Non-Ionizing Radiation, Part 1: Static and Extremely Low-Frequency (ELF) Electric and Magnetic Fields*. IARC Monographs on the Evaluation of Carcinogenic Risks to Humans, 2002, no. 80, p. 395.
3. *Standard of Building Biology Testing Methods: SBM–2015*. Germany: Institut für Baubiologie + Ekologie IBN, 2015, 5 p. Available at: <https://buildingbiology.com/building-biology-standard> (Accessed 01 February 2024).
4. Milutinov M., Juhas A., Pekarić-Nadž N. Magnetic field of electrical radiant heating system. *Safety Engineering*, 2017, vol. 7, no. 2, pp. 61–65. doi: <https://doi.org/10.7562/SE2017.7.02.03>.
5. *DBN V.2.5-24:2012. State building regulations of Ukraine. Electrical cable scorching system*. Kyiv, Minrehionbud Publ., 2012. 81 p. (Ukr).
6. *SOU-N EE 20.179:2008. Calculation of electric and magnetic fields of power lines. Methodology (with changes) (in the edition of the order of the Minenergugillya dated July 1, 2016, no. 423)*. Kyiv, Minenergugillya Ukraine Publ., 2016. 37 p. (Ukr).
7. Conti R., Giorgi A., Rendina R., Sartore L., Sena E.A. Technical solutions to reduce 50 hz magnetic fields from power lines. *2003 IEEE Bologna Power Tech Conference Proceedings*, 2003, vol. 2, pp. 1016–1021. doi: <https://doi.org/10.1109/PTC.2003.1304685>.
8. *SOU-N MEV 40.1-37471933-49:2011. Design of cable lines up to 330 kV. Guideline (in the edition of the order of the Minenergugillya dated January 26, 2017 no. 82)*. Kyiv, Minenergugillya Ukraine Publ., 2017. 168 p. (Ukr).

9. Nesterenko A.D. *Introduction to Theoretical Electrical Engineering*. Kyiv, Naukova Dumka Publ., 1969. 351 p. (Rus).
10. Shimoni K. *Theoretical Electrical Engineering (translation from German)*. Moscow, Mir Publ., 1964. 774 p. (Rus).
11. DSNiP 3.3.6.096-2002. *State sanitary standards and rules for working with sources of electromagnetic fields (order of the Ministry of Health (MoH) of Ukraine dated December 18, 2002 no. 476)*. Kyiv, MoH Publ., 2003. 16 p. (Ukr).
12. World Health Organization. *Electromagnetic fields and public health. Exposure to extremely low frequency fields*. Available at: <https://www.who.int/teams/environment-climate-change-and-health/radiation-and-health/non-ionizing/exposure-to-extremely-low-frequency-field> (Accessed 01 February 2024).
13. Tognola G., Chiamarello E., Bonato M., Magne I., Souques M., Fiocchi S., Parazzini M., Ravazzani P. Cluster Analysis of Residential Personal Exposure to ELF Magnetic Field in Children: Effect of Environmental Variables. *International Journal of Environmental Research and Public Health*, 2019, vol. 16, no. 22, art. no. 4363. doi: <https://doi.org/10.3390/ijerph16224363>.
14. Wertheimer N., Leeper E. Electrical wiring configurations and childhood cancer. *American Journal of Epidemiology*, 1979, vol. 109, no. 3, pp. 273-284. doi: <https://doi.org/10.1093/oxfordjournals.aje.a112681>.
15. Kheifets L., Ahlbom A., Crespi C.M., Draper G., Hagihara J., Lowenthal R.M., Mezei G., Oksuzyan S., Schüz J., Swanson J., Tittarelli A., Vinceti M., Wunsch Filho V. Pooled analysis of recent studies on magnetic fields and childhood leukaemia. *British Journal of Cancer*, 2010, vol. 103, no. 7, pp. 1128-1135. doi: <https://doi.org/10.1038/sj.bjc.6605838>.
16. Green L.M., Miller A.B., Villeneuve P.J., Agnew D.A., Greenberg M.L., Li J., Donnelly K.E. A case-control study of childhood leukemia in Southern Ontario, Canada, and exposure to magnetic fields in residences. *International Journal of Cancer*, 1999, vol. 82, no. 2, pp. 161-170. doi: [https://doi.org/10.1002/\(SICI\)1097-0215\(19990719\)82:2<161::AID-IJC2>3.0.CO;2-X](https://doi.org/10.1002/(SICI)1097-0215(19990719)82:2<161::AID-IJC2>3.0.CO;2-X).
17. Guidelines for Limiting Exposure to Time-Varying Electric and Magnetic Fields (1 Hz to 100 kHz). *Health Physics*, 2010, vol. 99, no. 6, pp. 818-836. doi: <https://doi.org/10.1097/HP.0b013e3181f06c86>.
18. Sage C., Carpenter D.O. *BioInitiative Report: A Rationale for Biologically-based Exposure Standards for Low-Intensity Electromagnetic Radiation*. BioInitiative Working Group. 2012. 1479 p. Available at: [https://www.infrastructure.gov.au/sites/default/files/submissions/BioInitiative Working Group.pdf](https://www.infrastructure.gov.au/sites/default/files/submissions/BioInitiative%20Working%20Group.pdf) (Accessed 01 February 2024).
19. World Health Organization. *Exposure limits for low-frequency fields (public). Data by country*. Available at: <https://apps.who.int/gho/data/node.main.EMFLIMITSPUBLICLOW?lang=en> (Accessed 01 February 2024).
20. Kuznetsov B.I., Nikitina T.B., Bovdii I.V., Voloshko O.V., Kolomiets V.V., Kobylianskyi B.B. Synthesis of an effective system of active shielding of the magnetic field of a power transmission line with a horizontal arrangement of wires using a single compensation winding. *Electrical Engineering & Electromechanics*, 2022, no. 6, pp. 15-21. doi: <https://doi.org/10.20998/2074-272X.2022.6.03>.
21. Kuznetsov B.I., Kutsenko A.S., Nikitina T.B., Bovdii I.V., Kolomiets V.V., Kobylianskyi B.B. Method for design of two-level system of active shielding of power frequency magnetic field based on a quasi-static model. *Electrical Engineering & Electromechanics*, 2024, no. 2, pp. 31-39. doi: <https://doi.org/10.20998/2074-272X.2024.2.05>.
22. Rozov V.Y., Reutskiy S.Y., Kundius K.D. Protection of workers against the magnetic field of 330-750 kV overhead power lines when performing work without removing the voltage under load. *Electrical Engineering & Electromechanics*, 2024, no. 4, pp. 70-78. doi: <https://doi.org/10.20998/2074-272X.2024.4.09>.
23. Rozov V.Y., Reutskiy S.Y., Pelevin D.Y., Kundius K.D. Approximate method for calculating the magnetic field of 330-750 kV high-voltage power line in maintenance area under voltage. *Electrical Engineering & Electromechanics*, 2022, no. 5, pp. 71-77. doi: <https://doi.org/10.20998/2074-272X.2022.5.12>.
24. Rozov V.Y., Pelevin D.Y., Kundius K.D. Simulation of the magnetic field in residential buildings with built-in substations based on a two-phase multi-dipole model of a three-phase current conductor. *Electrical Engineering & Electromechanics*, 2023, no. 5, pp. 87-93. doi: <https://doi.org/10.20998/2074-272X.2023.5.13>.
25. Rozov V.Yu., Rezinkina M.M., Dumanskiy Yu.D., Gvozdenko L.A. The study of man-caused distortions in the geomagnetic field of residential and industrial buildings and to identify ways to reduce them to a safe level. *Technical Electrodynamics. Thematic Issue «Problems of Modern Electrical Engineering»*, 2008, chapter 2, pp. 3-8. (Rus).
26. Rozov V.Yu. To the 40th anniversary of the Science and Technology Center of Magnetism of Technical Objects of the NAS of Ukraine. *Technical Electrodynamics*, 2010, no. 3, pp. 74-80. (Rus).
27. Baranov M.I., Rozov V.Y., Sokol Y.I. To the 100th anniversary of the National academy of sciences of Ukraine – the cradle of domestic science and technology. *Electrical Engineering & Electromechanics*, 2018, no. 5, pp. 3-11. doi: <https://doi.org/10.20998/2074-272X.2018.5.01>.
28. Rozov V.Yu., Getman A.V., Petrov S.V. Magnetism of space-craft. *Technical Electrodynamics. Thematic Issue «Problems of Modern Electrical Engineering»*, 2010, chapter 2, pp. 144-147. (Rus).
29. Rozov V., Grinchenko V., Tkachenko O., Yerisov A. Analytical Calculation of Magnetic Field Shielding Factor for Cable Line with Two-Point Bonded Shields. *2018 IEEE 17th International Conference on Mathematical Methods in Electromagnetic Theory (MMET)*, 2018, pp. 358-361. doi: <https://doi.org/10.1109/MMET.2018.8460425>.
30. Dumanskiy V.Yu., Serdyuk A.M., Los' I.P. *The influence of electromagnetic radiation on humans*. Kyiv, Zdorovye Publ., 1975. 180 p. (Rus).
31. Dumanskiy V., Bitkin S., Didyk N., Dumanskiy Yu., Nikitina N., Mzyuk M., Bezverkha A., Zotov S., Tomashevskaya L., Semashko P., Lyashenko V., Galak S., Medvedev S. Hygienical ground of requirements to placing and exploitation of cable busses of electricity transmission and their equipment in the conditions of modern municipal building. *Hygiene of populated places*, 2015, no. 66, pp. 20-29. (Ukr).
32. *Electrical installation regulations*. Kharkiv, Fort Publ., 2017. 760 p. (Ukr).
33. *SunTouch Heating Mat Kits*. Available at: <https://www.flooringsupplyshop.com/category/suntouch-heating-mats-kits-119> (Accessed 01 February 2024).
34. *Arnold Rak*. Available at: www.rak-waermetech.de (Accessed 01 February 2024).
35. *Hemstedt*. Available at: <https://www.hemstedt.de> (Accessed 01 February 2024).
36. *Handbook for Comfortable Warm Floors. nVent Raychem*. 2022. 48 p. Available at: https://www.nvent.com/sites/default/files/acquidam_assets/2022-08/RAYCHEM-TH-EU1001-Floorheating-EN.pdf (Accessed 01 February 2024).
37. *ELEKTRA Heating Cables. Installation manual*. 72 p. Available at: https://elektra.pl/download/ru/electrical-heating-systems/floor-heating/heating-cables-VCD/vcd7_vcd10_vcd17_heating_cables_manual.pdf (Accessed 01 February 2024).

38. Woks. PJSC «Odeskabel». Available at: <https://woks.ua/ua> (Accessed 01 February 2024).
39. *Indoor Cable Floor Heating Systems. Application manual.* 2016. 52 p. Available at: <https://assets.danfoss.com/documents/89845/AB213486470188en-010101.pdf> (Accessed 01 February 2024).
40. *VOLTERM Coaxial Heating system.* Available at: <https://volterm.com.ua> (Accessed 01 February 2024).
41. *3HeatTech. Radiant Floor Heating Cable.* Available at: <https://www.heattechproducts.com/electric-radiant-floor-heating-cable-kits> (Accessed 01 February 2024).
42. Ambartsumyants K. Heating cables: construction and applications. (Rus). Available at: <https://aw-therm.com.ua/nagrevatelnye-kabeli-konstrukciya-i-primenenie> (Accessed 01 June 2024).
43. Manilov A.M., Krasnozhon A.V., Tovstiuik S.O. Assessment of the magnitude of the magnetic field of cable heating of residential and industrial premises from the point of view of its safety for people. *Promelektro*, 2022, no. 3-6, pp. 32-36. (Ukr). Available at: <https://pdf.lib.vntu.edu.ua/books/2022/EP/Promelektro-3-6-2022.pdf> (Accessed 01 February 2024).
44. Thieblemont H., Haghghat F., Moreau A. Thermal Energy Storage for Building Load Management: Application to Electrically Heated Floor. *Applied Sciences*, 2016, vol. 6, no. 7, art. no. 194. doi: <https://doi.org/10.3390/app6070194>.
45. Gołębiowski J., Forenc J. The influence of side thermal insulation on distribution of the temperature field in an electrical floor heater. *Przegląd Elektrotechniczny*, 2016, no. 12, pp. 271-277. doi: <https://doi.org/10.15199/48.2016.12.68>.
46. Stratton J.A. *The Theory of Electromagnetism.* Moscow, Gostehizdat Publ., 1948. 520 p. (Rus).
47. Smythe W.R. *Static and Dynamic Electricity.* McGraw-Hill, New York, 1968. 623 p.

How to cite this article:

Rozov V.Yu., Reutskiy S.Yu., Pelevin D.Ye., Kundius K.D. Magnetic field of electrical heating cable systems of the floors for residential premises. *Electrical Engineering & Electromechanics*, 2024, no. 5, pp. 48-57. doi: <https://doi.org/10.20998/2074-272X.2024.5.07>

48. Kyessayev A.G. Impact on the transmission parameters eccentricity and ellipticity RF coaxial cables. *Bulletin of the National Technical University «KhPI». Series: Energy: Reliability and Energy Efficiency*, 2013, no. 59, pp. 62-69. (Ukr).
49. Bezprozvannykh G.V., Boyko A.M., Kessaev O.G. Influence of constructive and technological defects on coaxial radio-frequency cable impedance. *Electrical Engineering & Electromechanics*, 2013, no. 2, pp. 57-61. (Ukr).
50. Dwight H.B. *Tables of Integrals and Other Mathematical Data.* 4th ed. The Macmillan Company, 1972. 336 p.
51. Del Pino López J.C., Cruz Romero P., Dular P. Parametric analysis of magnetic field mitigation shielding for underground power cables. *Renewable Energy and Power Quality Journal*, 2007, vol. 1, no. 5, pp. 519-526. doi: <https://doi.org/10.24084/repqj05.326>.

Received 27.03.2024

Accepted 22.05.2024

Published 20.08.2024

V.Yu. Rozov¹, Doctor of Technical Science, Professor,
Corresponding member of NAS of Ukraine,
S.Yu. Reutskiy¹, PhD, Senior Researcher,
D.Ye. Pelevin¹, PhD, Senior Researcher,
K.D. Kundius¹, PhD,

¹ Anatolii Pidhornyi Institute of Mechanical Engineering
Problems of the National Academy of Sciences of Ukraine,
2/10, Pozharskogo Str., Kharkiv, 61046, Ukraine,
e-mail: vyurozov@gmail.com (Corresponding Author);
sergiyreutskiy@gmail.com; pelevindmitro@ukr.net;
kundiuckateryna@ukr.net